Electronic Supplementary Material (ESI) for Inorganic Chemistry Frontiers.
This journal is © the Partner Organisations 2019

Electronic Supplementary Information

Experimental Section

Materials: Bulk TiS_2 powders, Para-(dimethylamino) benzaldehyde ($C_9H_{11}NO$), sodium nitroferricyanide (III) dihydrate ($Na_2Fe(CN)_5NO{\cdot}2H_2O$), hydrogen peroxide ($H_2O_2$) and Nafion (5 wt%) were purchased from Aladdin Ltd. (Shanghai, China). Isopropyl alcohol (IPA), Sulfuric acid (H_2SO_4), ammonium chloride (NH_4Cl), hydrazine hydrate ($N_2H_4{\cdot}H_2O$), sodium hypochlorite (NaClO), sodium hydroxide (NaOH), sodium salicylate ($C_7H_5O_3Na$), sodium sulfate (Na_2SO_4), hydrochloric acid (HCl), ethanol (CH_3CH_2OH) and carbon paper were bought from Beijing Chemical Corporation. The water used throughout all experiments was purified through a Millipore system.

Preparation of TiS_2 NSs/CP electrode: Bulk TiS_2 powders were added to IPA (10 mL in a 14 mL vial) with an initial concentration of 7.5 mg/mL. These were sonicated using the point probe (sonic tip) for 90 minutes, with a nominal power output of 285 W (38%×750 W). After sonication, the dispersions were allowed to settle for 24 hours before centrifuging them at 1500 rpm for 45 minutes. The top 3/4 of the dispersion was collected by pipette. Next, 40 μL of 5 wt% Nafion was added into 960 μL of the obtained solution and sonicated for 1 h to form a homogeneous ink. Then, 140 μL of the dispersion was loaded onto a carbon paper electrode with area of 1 × 1 cm^2 and dried under ambient conditions, the catalyst loading mass is 0.1 mg cm^{-2}.

Characterizations: XRD data were recorded using a Shimazu XRD-6100 diffractometer with Cu Kα radiation (40 kV, 30 mA) of wavelength 0.154 nm (SHIMADZU, Japan). SEM images were obtained from a tungsten lamp-equipped SU3500 scanning electron microscope at an accelerating voltage of 20 kV (HITACHI, Japan). TEM images were collected from a HITACHI H-8100 electron microscopy (Hitachi, Tokyo, Japan) operated at 200kV. XPS data were acquired on an ESCALABMK II X-ray photoelectron spectrometer using Mg as the exciting source. The absorbance data of spectrophotometer were measured on SHIMADZU UV–1800 ultraviolet-visible (UV–Vis) spectrophotometer. A gas

chromatography (SHIMADZU, GC-2014C) equipped with MolSieve 5A column and Ar carrier gas was used for H_2 quantifications. Gas-phase product was sampled every 600 s using a gas-tight syringe (Hamilton). The ion chromatography data were collected on 930 Compact IC Flex (Metrohm, Switzerland). The ion chromatography data were collected on Thermofisher ICS 5000 plus using the dual temperature heater, injection valve, conductivity detector, AERS 500 Anions suppressor.

Electrocatalytic N_2 reduction measurements: The N_2 reduction experiments were carried out in a two-compartment cell under ambient condition, which was separated by Nafion 117 membrane. The membrane was treated in H_2O_2 (5%) aqueous solution at 80 °C for 1 h and dipped in 0.1 M H_2SO_4 at 80°C for another 1 h. Finally, the membrane was treated in ultrapure water at 80°C overnight. The electrochemical experiments were performed with a CHI 660E electrochemical analyzer using a three-electrode configuration with TiS_2 NS/CP electrode, graphite rod and Ag/AgCl electrode (saturated KCl electrolyte) as working electrode, counter electrode and reference electrode, respectively. In all measurements, saturated Ag/AgCl electrode was calibrated with respect to reversible hydrogen electrode as following: E (vs. RHE) = E (vs. Ag/AgCl) + 0.059 × pH + 0.197 V. The presented current density was normalized to the geometric surface area. For electrochemical N_2 reduction, chronoamperometry tests were conducted in N_2-saturated 0.1 M Na_2SO_4 solution (30mL). All experiments were carried out under room temperature.

Determination of NH_3: The produced NH_3 was detected with indophenol blue by ultraviolet spectroscopy.[1] In detail, 4 mL electrolyte was obatined from the cathodic chamber and mixed with 50 μL oxidizing solution containing NaClO (4.5%) and NaOH (0.75 M), 500 μL coloring solution containing 0.4 M $C_7H_6NaO_3$ and 0.32 M NaOH, and 50 μL catalyst solution (1 wt % $Na_2Fe(CN)_5NO{\cdot}2H_2O$) for 1 h in dark. Absorbance measurements were performed at λ = 660 nm. The concentration absorbance curve was calibrated using standard NH_4^+ solution with a serious of

concentrations. The fitting curve ($y = 0.510x + 0.011$, $R^2 = 0.998$) shows good linear relation of absorbance value with NH_4^+ concentration.

Determination of N_2H_4: The N_2H_4 present in the electrolyte was determined by the method of Watt and Chrisp.[2] The mixture of $C_9H_{11}NO$ (5.99 g), HCl (concentrated, 30 mL), and C_2H_5OH (300 mL) was used as a color reagent. In detail, 5 mL electrolyte was removed from the electrochemical reaction vessel, and added into 5 mL above prepared color reagent for 10 min at room temperature. Moreover, the absorbance of the resulting solution was measured at a wavelength of 455 nm. The concentration absorbance curves were calibrated using standard N_2H_4 solution with a series of concentrations. The fitting curve ($y = 0.719x + 0.051$, $R^2 = 0.999$) shows good linear relation of absorbance value with N_2H_4 concentration.

Determination of FE and V_{NH_3}: The Faradaic efficiency (FE) for N_2 reduction was defined as the amount of electric charge used for synthesizing NH_3 divided the total charge passed through the electrodes during the electrolysis. The total amount of NH_3 produced was measured using colorimetric methods. Assuming three electrons were needed to produce one NH_3 molecule, the FE could be calculated as follows:

$$FE = \frac{3F \times [NH_4^+] \times V}{18 \times Q}$$

The rate of NH_3 formation was calculated using the following equation:

$$V_{NH_3} = \frac{[NH_4^+] \times V}{t \times m_{cat.}}$$

Where F is the Faraday constant, $[NH_4^+]$ is the measured NH_4^+ concentration, V is the volume of the electrolyte in the cathodic chamber, Q is the total quantity of applied electricity; t is the reduction time; $m_{cat.}$ is the loaded mass of catalyst on carbon paper.

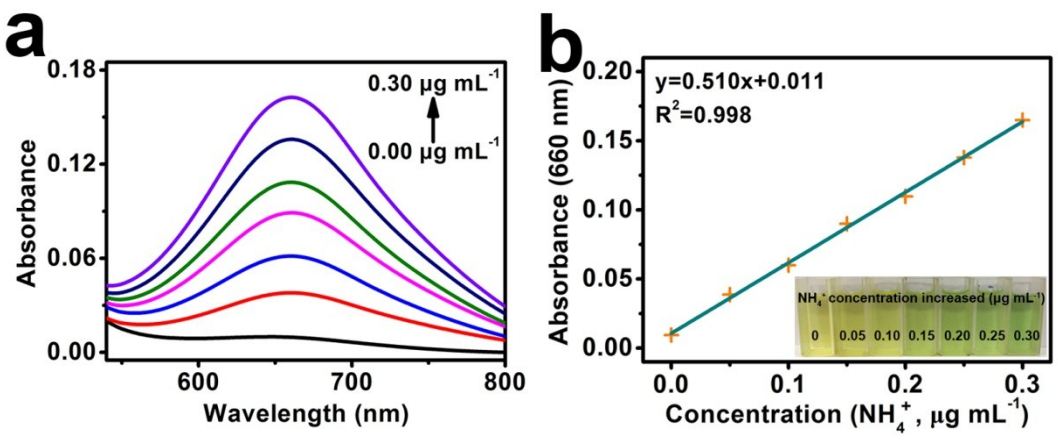

Fig. S1. (a) UV–vis absorption spectra of various NH_4^+ concentrations after incubated for 2 hours at room temperature. (b) Calibration curve used for calculation of NH_4^+ concentrations.

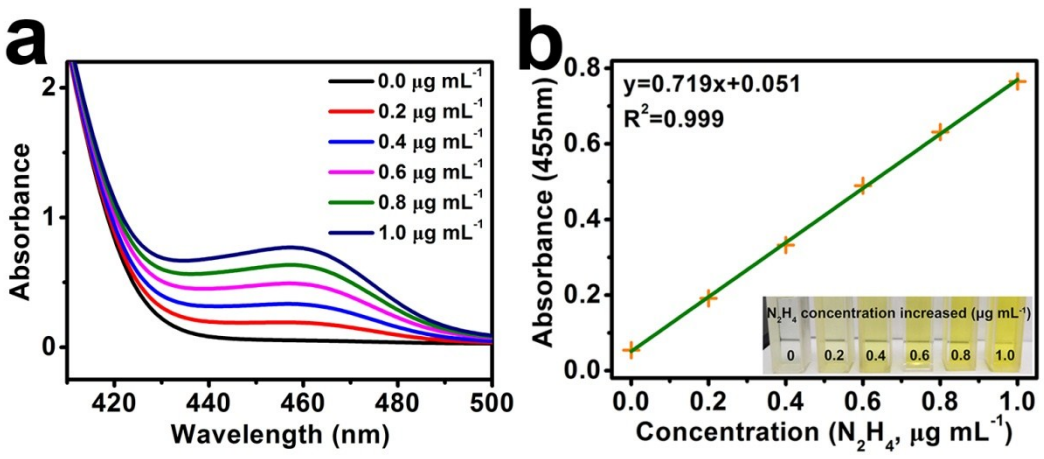

Fig. S2. (a) UV–vis absorption spectra of various N_2H_4 concentrations after incubated for 20 min at room temperature. (b) Calibration curve used for calculation of N_2H_4 concentrations.

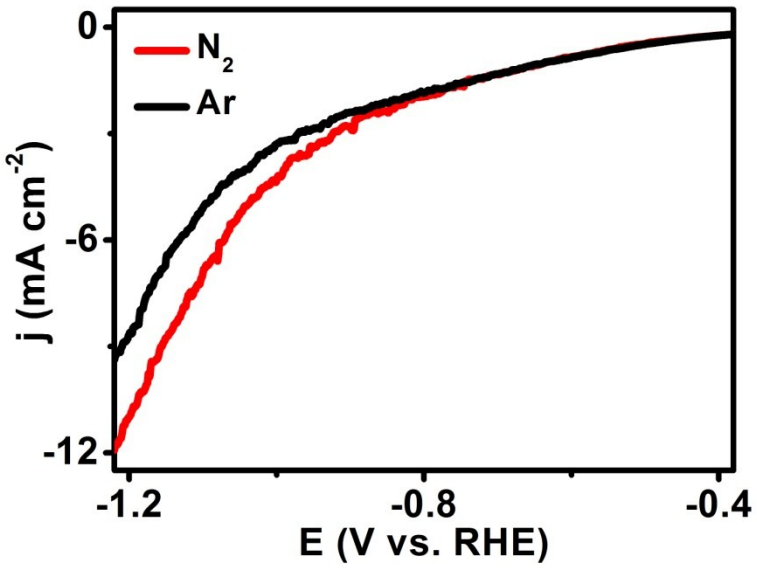

Fig. S3. LSV curves of TiS_2 NSs/CP in Ar- and N_2-saturated 0.1 M Na_2SO_4 with a scan rate of 2 mV s^{-1}.

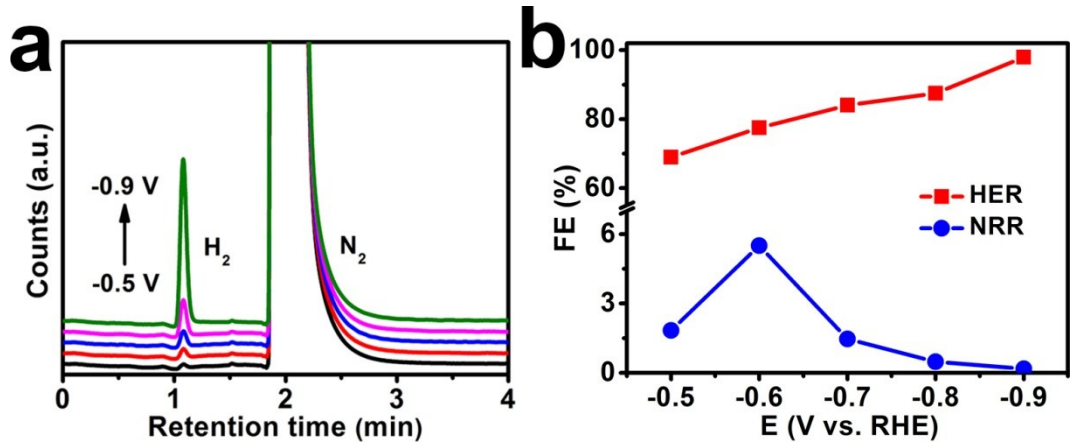

Fig. S4. (a) gas chromatography (GC) spectra of the gas from on-line measurements collected by GC for the NRR on TiS_2 NSs/CP in N_2-saturated 0.1 M Na_2SO_4 at various potentials. The on-line measurements were collected every 10 minutes. (b) The calculated FEs of HER and NRR at various potentials.

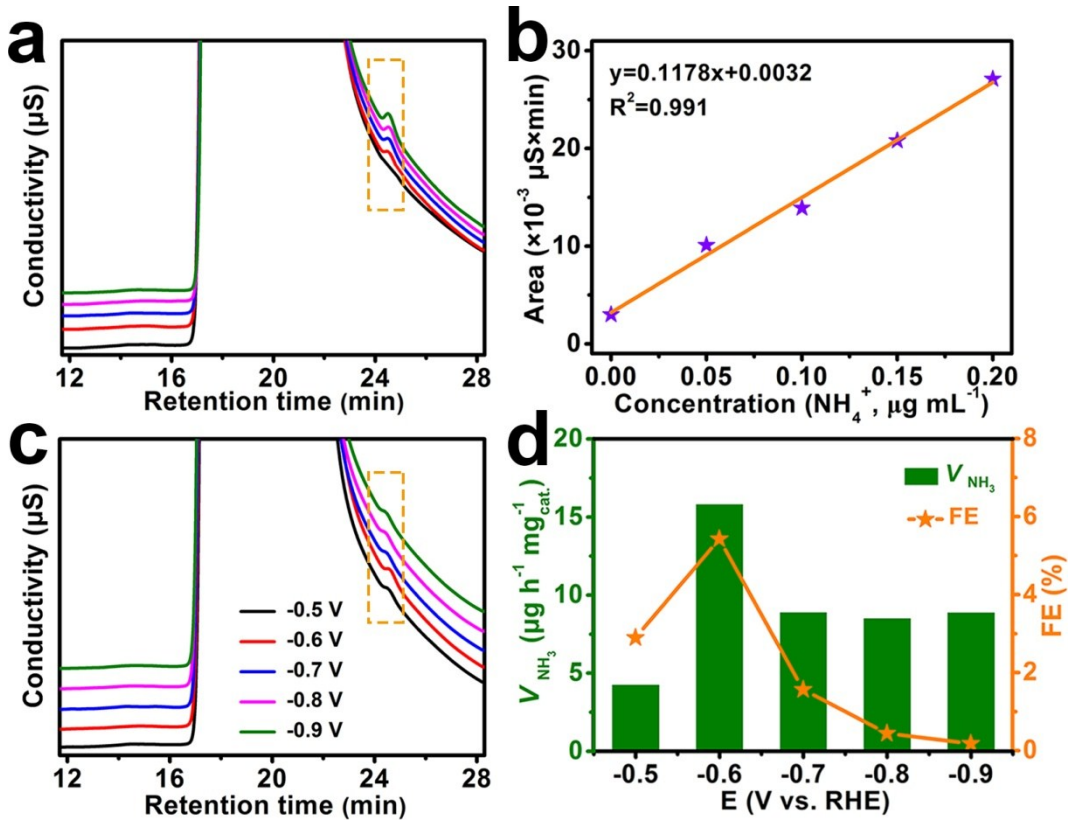

Fig. S5. (a) Ion chromatogram analysis for the NH_4^+ ions. (b) Calibration curve used for estimation of NH_4^+. (c) Ion chromatogram for the electrolytes at a series of potentials after electrolysis for 2 h. (d) NH_3 yields and FEs for TiS_2 NSs/CP at corresponding potentials.

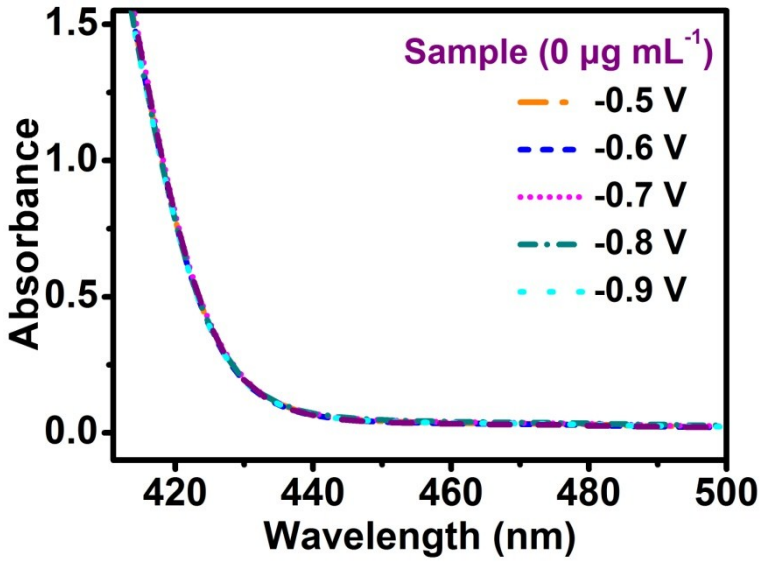

Fig. S6. UV–vis spectra of the electrolyte estimated by the method of Watt and Chrisp before and after 2 h electrolysis in N_2 atmosphere at a series of potentials under ambient conditions.

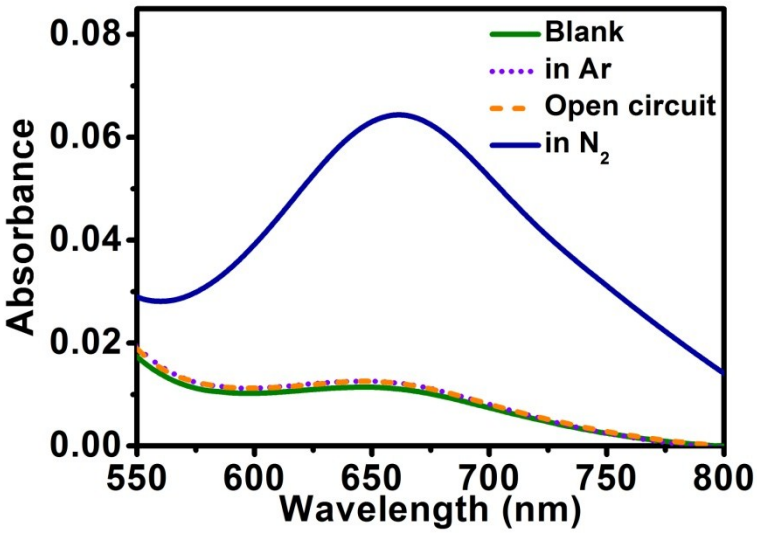

Fig. S7. UV–vis absorption spectra of the electrolyte stained with indophenol indicator after charging at –0.6 V for 2 h under different electrochemical conditions.

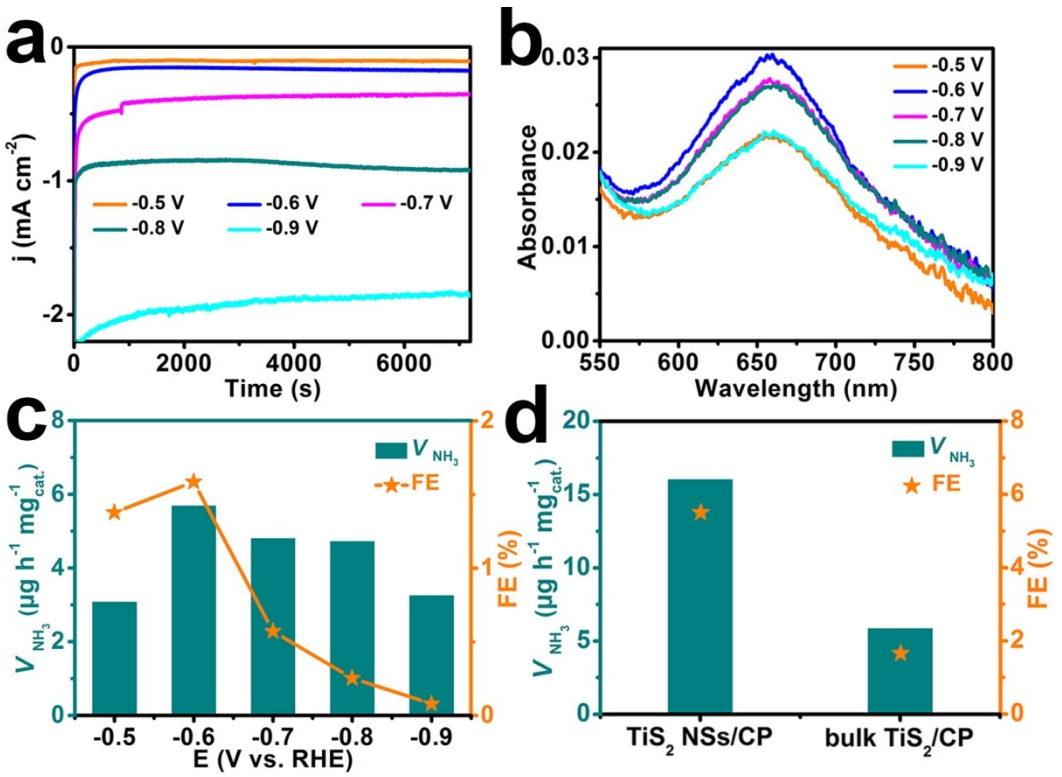

Fig. S8. (a) Time-dependent current density curves for bulk TiS_2/CP at different potentials in N_2-saturated 0.1 M Na_2SO_4. (b) UV–vis absorption spectra of the electrolytes stained with indophenol indicator after electrolysis at a series of potentials for 2 h. (c) NH_3 yields and FEs of bulk TiS_2/CP for NRR at a series of potentials. (d) NH_3 yields and FEs with different electrodes at –0.6 V after 2 h electrolysis under ambient conditions.

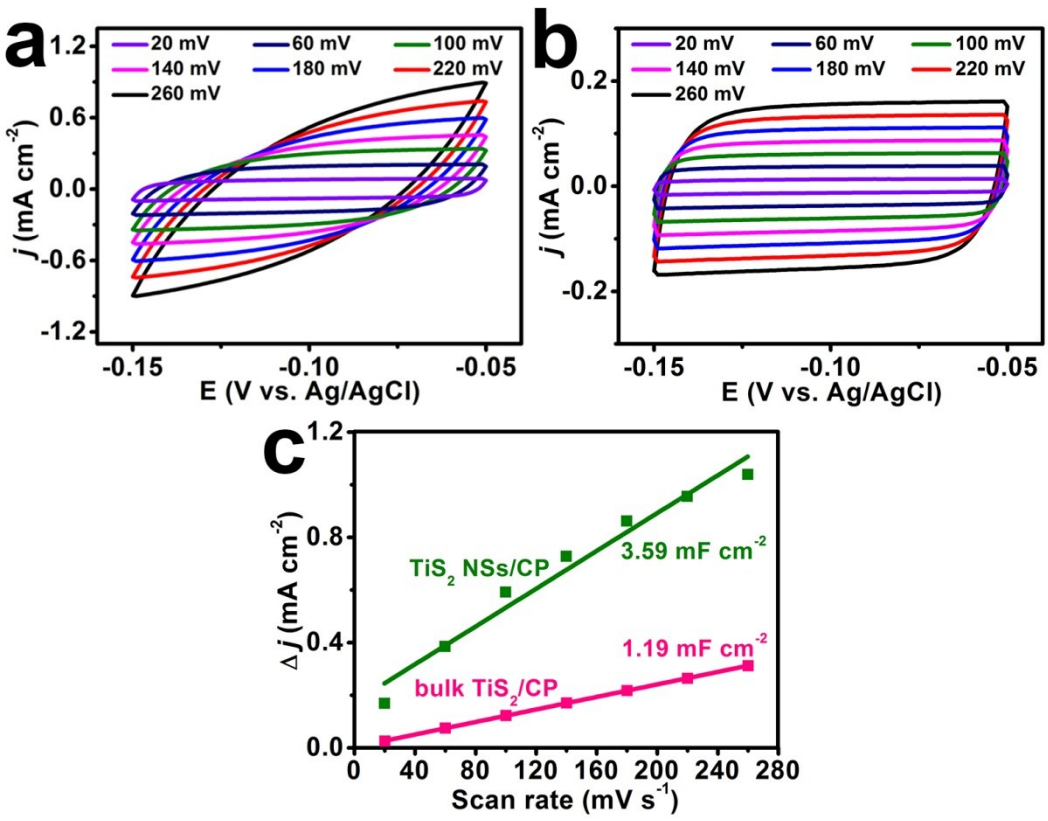

Fig. S9. Cyclic voltammetry curves of (a) TiS_2 NSs/CP and (b) bulk TiS_2/CP with various scan rates (20-260 mV s^{-1}) in the region of –0.05 to –0.15 V vs. Ag/AgCl. (c) The capacitive current densities at –0.10 V vs. Ag/AgCl as a function of scan rates for TiS_2 NSs/CP and bulk TiS_2/CP.

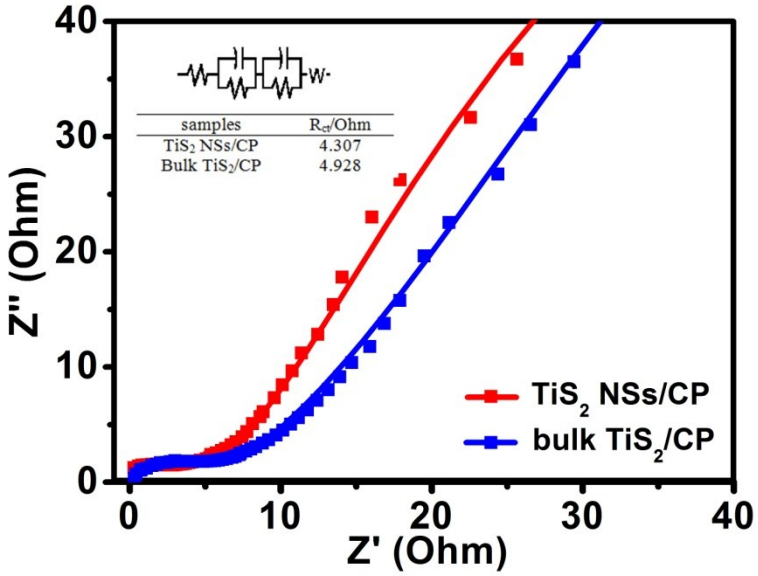

Fig. S10. Nyquist plots and fitting lines of TiS_2 NSs/CP and bulk TiS_2/CP with a voltage amplitude of 5 mV, and all three electrodes are in one compartment cell being full of 0.1 M Na_2SO_4 solution.

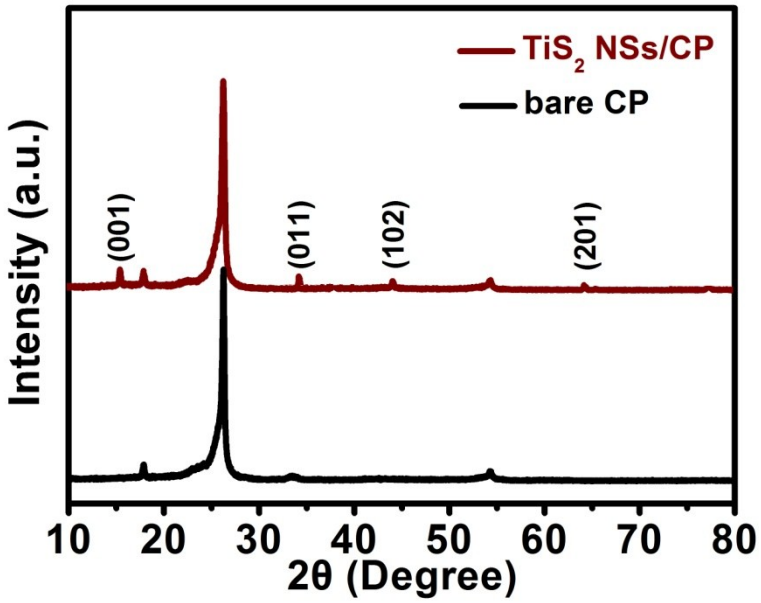

Fig. S11. XRD patterns for TiS_2 NSs/CP and bare CP after long-term electrocatalysis in 0.1 M Na_2SO_4.

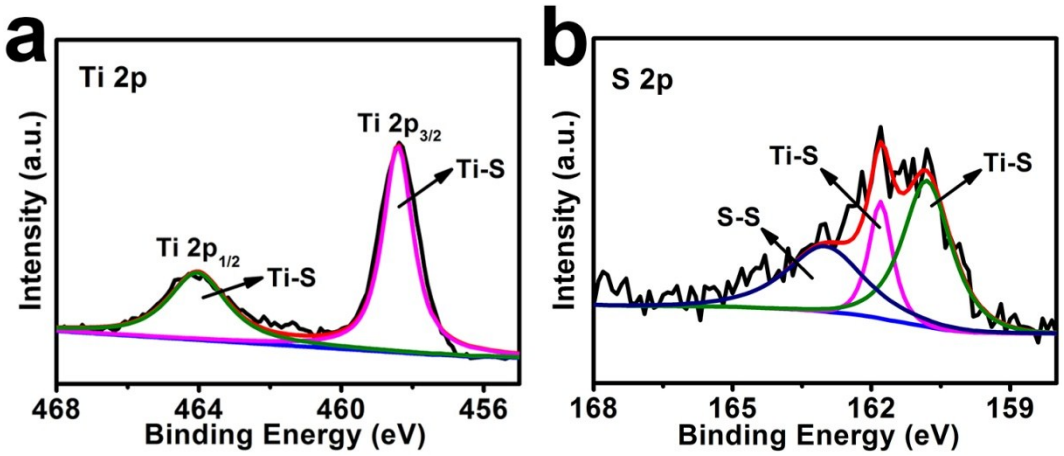

Fig. S12. XPS spectra for TiS_2 NSs/CP in the (a) Ti 2p, (b) S 2p regions after long-term electrocatalysis in 0.1 M Na_2SO_4.

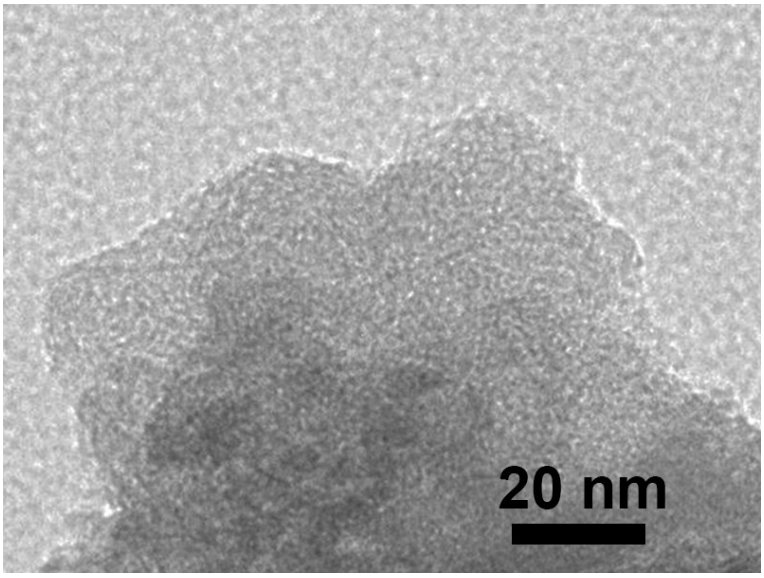

Fig. S13. TEM image for TiS_2 NSs after long-term electrocatalysis in 0.1 M Na_2SO_4.

Table S1. Comparison of ambient N_2 reduction performance for TiS_2 nanosheets with other aqueous-based NRR electrocatalysts.

Catalyst	Electrolyte	NH_3 yield	FE (%)	Ref.
TiS_2 NSs	0.1 M Na_2SO_4	16.02 μg h^{-1} $mg^{-1}_{cat.}$	5.50	This work
MoS_2/CC	0.1 M Na_2SO_4	8.08×10^{-11} mol s^{-1} cm^{-2}	1.17	3
TiO_2	0.1 M Na_2SO_4	9.16×10^{-11} mol $s^{-1} \cdot cm^{-2}$	2.5	4
TiO_2-rGO	0.1 M Na_2SO_4	15.13 μg h^{-1} $mg^{-1}_{cat.}$	3.3	5
C-TiO_2	0.1 M Na_2SO_4	16.22 μg h^{-1} $mg^{-1}_{cat.}$	1.84	6
B-TiO_2	0.1 M Na_2SO_4	14.4 μg h^{-1} $mg^{-1}_{cat.}$	3.4	7
defect-rich MoS_2 nanoflower	0.1 M Na_2SO_4	29.28 μg h^{-1} $mg^{-1}_{cat.}$	8.34	8
d-TiO_2/TM	0.1 M HCl	1.24×10^{-10} mol s^{-1} cm^{-2}	9.17	9
N-doped porous carbon	0.05 M H_2SO_4	23.8 μg h^{-1} $mg^{-1}_{cat.}$	1.42	10
Mo nanofilm	0.01 M H_2SO_4	3.09×10^{-11} mol s^{-1} cm^{-2}	0.72	11
γ-Fe_2O_3	0.1 M KOH	0.212 μg h^{-1} $mg^{-1}_{cat.}$	1.9	12
$Pd_{0.2}Cu_{0.8}$/rGO	0.1 M KOH	1.66 μg h^{-1} $mg^{-1}_{cat.}$	4.5	13
Fe_2O_3 nanorods	0.1 M Na_2SO_4	15.9 μg h^{-1} $mg^{-1}_{cat.}$	0.94	14
PEBCD/C	0.5 M Li_2SO_4	1.58 μg h^{-1} cm^{-2}	2.85	15
Fe_2O_3-CNT	$KHCO_3$	0.22 μg h^{-1} cm^{-2}	0.15	16
Au nanorods	0.1 M KOH	6.042 μg h^{-1} $mg^{-1}_{cat.}$	4.0	17
TA-reduced Au/TiO_2	0.1 M HCl	21.4 μg h^{-1} $mg^{-1}_{cat.}$	8.11	18
α-Au/CeO_x-RGO	0.1 M HCl	8.31 μg h^{-1} $mg^{-1}_{cat.}$	10.10	19
MoN	0.1 M HCl	3.01×10^{-10} mo1 s^{-1} cm^{-2}	1.15	20
Ru/C	2.0 M KOH	0.25 μg h^{-1} cm^{-2}	0.92	21
Fe_3O_4/Ti	0.1 M Na_2SO_4	5.6×10^{-11} mol s^{-1} cm^{-2}	2.6	22
$Bi_4V_2O_{11}$/CeO_2	0.1 M HCl	23.21 μg h^{-1} $mg^{-1}_{cat.}$	10.16	23
MoO_3	0.1 M HCl	29.43 μg h^{-1} $mg^{-1}_{cat.}$	1.9	24

VN	0.1 M HCl	8.40×10^{-11} mol s^{-1} cm^{-2}	2.25	25
Nb_2O_5 nanofiber	0.1 M HCl	43.6 μg h^{-1} $mg^{-1}_{cat.}$	9.26	26
Mn_3O_4 nanocube	0.1 M Na_2SO_4	11.6 μg h^{-1} $mg^{-1}_{cat.}$	3.0	27
$Ti_3C_2T_x$ nanosheet	0.1 M HCl	20.4 μg h^{-1} $mg^{-1}_{cat.}$	9.3	28
MnO	0.1 M Na_2SO_4	1.11×10^{-10} mol s^{-1} cm^{-2}	8.02	29
AuSAs-NDPCs	0.1 M HCl	2.32 μg h^{-1} cm^{-2}	12.3	30
AuHNCs	0.5 M $LiClO_4$	3.98 μg h^{-1} cm^{-2}	14.8	31
B_4C	0.1 M HCl	26.57 μg h^{-1} $mg^{-1}_{cat.}$	15.95	32
hollow Cr_2O_3 microspheres	0.1 M Na_2SO_4	25.3 μg h^{-1} $mg^{-1}_{cat.}$	6.78	33
Ag nanosheets	0.1 M HCl	4.62×10^{-11} mol s^{-1} cm^{-2}	4.8	34
β-FeOOH nanorods	0.5 M $LiClO_4$	23.32 μg h^{-1} $mg^{-1}_{cat.}$	6.7	35
SnO_2	0.1 M Na_2SO_4	1.47×10^{-10} mol s^{-1} cm^{-2}	2.17	36
porous bromide-derived Ag film	0.1 M Na_2SO_4	2.07×10^{-11} mol s^{-1} cm^{-2}	7.36	37
S-doped carbon nanospheres	0.1 M Na_2SO_4	19.07 μg h^{-1} $mg^{-1}_{cat.}$	7.47	38
oxygen-doped carbon nanosheet	0.1 M HCl	20.15 μg h^{-1} $mg^{-1}_{cat.}$	4.97	39
Nb_2O_5 nanowires array/CC	0.1 M Na_2SO_4	1.58×10^{-10} mol s^{-1} cm^{-2}	2.26	40
VO_2 hollow microsphere	0.1 M Na_2SO_4	14.85 μg h^{-1} $mg^{-1}_{cat.}$	3.97	41
Ru SAs/N-C	0.05 M H_2SO_4	120.9 μg h^{-1} $mg^{-1}_{cat.}$	29.6	42
Au flowers	0.1 M HCl	25.57 μg h^{-1} $mg^{-1}_{cat.}$	6.05	43
NbO_2 nanoparticles	0.05 M H_2SO_4	11.6 μg h^{-1} $mg^{-1}_{cat.}$	19.7	44
Fe_3S_4 nanosheets	0.1 M HCl	75.4 μg h^{-1} $mg^{-1}_{cat.}$	6.45	45
La_2O_3	0.1 M Na_2SO_4	17.04 μg h^{-1} $mg^{-1}_{cat.}$	4.76	46
CoO quantum dots	0.1 M Na_2SO_4	21.5 μg h^{-1} $mg^{-1}_{cat.}$	8.3	47
Bi nanosheet array	0.1 M HCl	6.89×10^{-11} mol s^{-1} cm^{-2}	10.26	48

References

1 D. Zhu, L. Zhang, R. E. Ruther and R. J. Hamers, *Nat. Mater.*, 2013, **12**, 836–841.

2 G. W. Watt and J. D. Chrisp, *Anal. Chem.*, 1952, **24**, 2006–2008.

3 L. Zhang, X. Ji, X. Ren, Y. Ma, X. Shi, Z. Tian, A. M. Asiri, L. Chen, B. Tang and X. Sun, *Adv. Mater.*, 2018, **30**, 1800191.

4 R. Zhang, X. Ren, X. Shi, F. Xie, B. Zheng, X. Guo and X. Sun, *ACS Appl. Mater. Interfaces*, 2018, **10**, 28251–28255.

5 X. Zhang, Q. Liu, X. Shi, A. M. Asiri, Y. Luo, X. Sun and T. Li, *J. Mater. Chem. A*, 2018, **6**, 17303–17306.

6 K. Jia, Y. Wang, Q. Pan, B. Zhong, Y. Luo, G. Cui, X. Guo and X. Sun, *Nanoscale Adv.*, 2019, **1**, 961–964.

7 Y. Wang, K. Jia, Q. Pan, Y. Xu, Q. Liu, G. Cui, X. Guo and X. Sun, *ACS Sustainable Chem. Eng.*, 2019, **7**, 117–122.

8 X. Li, T. Li, Y. Ma, Q. Wei, W. Qiu, H. Guo, X. Shi, P. Zhang, A. M. Asiri, L. Chen, B. Tang and X. Sun, *Adv. Energy Mater.*, 2018, **8**, 1801357.

9 L. Yang, T. Wu, R. Zhang, H. Zhou, L. Xia, X. Shi, H. Zheng, Y. Zhang and X. Sun, *Nanoscale*, 2019, **11**, 1555–1562.

10 Y. Liu, Y. Su, X. Quan, X. Fan, S. Chen, H. Yu, H. Zhao, Y. Zhang and J. Zhao, *ACS Catal.*, 2018, **8**, 1186−1191.

11 D. Yang, T. Chen and Z. Wang, *J. Mater. Chem. A*, 2017, **5**, 18967–18971.

12 J. Kong, A. Lim, C. Yoon, J. H. Jang, H. C. Ham, J. Han, S. Nam, D. Kim, Y. Sung, J. Choi and H. S. Park, *ACS Sustainable Chem. Eng.*, 2017, **5**, 10986–10995.

13 M. Shi, D. Bao, S. Li, B. Wulan, J. Yan and Q. Jiang, *Adv. Energy Mater.*, 2018, **8**, 1800124.

14 X. Xiang, Z. Wang, X. Shi, M. Fan and X. Sun, *ChemCatChem*, 2018, **10**, 1–7.

15 G. Chen, X. Cao, S. Wu, X. Zeng, L. Ding, M. Zhu and H. Wang, *J. Am. Chem.*

Soc., 2017, **139**, 9771–9774.

16 S. Chen, S. Perathoner, C. Ampelli, C. Mebrahtu, D. Su and G. Centi, *Angew. Chem., Int. Ed.*, 2017, **56**, 2699–2703.

17 D. Bao, Q. Zhang, F. Meng, H. Zhong, M. Shi, Y. Zhang, J. Yan, Q. Jiang and X. Zhang, *Adv. Mater.*, 2017, **29**, 1604799.

18 M. Shi, D. Bao, B. Wulan, Y. Li, Y. Zhang, J. Yan and Q. Jiang, *Adv. Mater.*, 2017, **29**, 1606550.

19 S. Li, D. Bao, M. Shi, B. Wulan, J. Yan and Q. Jiang, *Adv. Mater.*, 2017, **29**, 1700001.

20 L. Zhang, X. Ji, X. Ren, Y. Luo, X. Shi, A. M. Asiri, B. Zheng and X. Sun, *ACS Sustainable Chem. Eng.*, 2018, **6**, 9550–9554.

21 V. Kordali, G. Kyriacou and C. Lambrou, *Chem. Commun.*, 2000, **17**, 1673–1674.

22 Q. Liu, X. Zhang, B. Zhang, Y. Luo, G. Cui, F. Xie and X. Sun, *Nanoscale*, 2018, **10**, 14386–14389.

23 C. Lv, C. Yan, G. Chen, Y. Ding, J. Sun, Y. Zhou and G. Yu, *Angew. Chem.*, *Int. Ed.*, 2018, **57**, 6073–6076.

24 J. Han, X. Ji, X. Ren, G. Cui, L. Li, F. Xie, H. Wang, B. Li and X. Sun, *J. Mater. Chem. A*, 2018, **6**, 12974–12977.

25 R. Zhang, Y. Zhang, X. Ren, G. Cui, A. M. Asiri, B. Zheng and X. Sun, *ACS Sustainable Chem. Eng.*, 2018, **6**, 9545–9549.

26 J. Han, Z. Liu, Y. Ma, G. Cui, F. Xie, F. Wang, Y. Wu, S. Gao, Y. Xu and X. Sun, *Nano Energy*, 2018, **52**, 264–270.

27 X. Wu, L. Xia, Y. Wang, W. Lu, Q. Liu, X. Shi and X. Sun, *Small*, 2018, **14**, 1803111.

28 J. Zhao, L. Zhang, X. Xie, X. Li, Y. Ma, Q. Liu, W. Fang, X. Shi, G. Cui and X. Sun, *J. Mater. Chem. A*, 2018, **6**, 24031–24035.

29 Z. Wang, F. Gong, L. Zhang, R. Wang, L. Ji, Q. Liu, Y. Luo, H. Guo, Y.

Li, P. Gao, X. Shi, B. Li, B. Tang and X. Sun, *Adv. Sci.*, 2018, **5**, 1801182.

30 Q. Qin, T. Heil, M. Antonietti and M. Oschatz, *Small Methods*, 2018, **2**, 1800202.

31 M. Nazemi, S. R. Panikkanvalappil and M. A. El-Sayed, *Nano Energy*, 2018, **49**, 316–323.

32 W. Qiu, X. Xie, J. Qiu, W. Fang, R. Liang, X. Ren, X. Ji, G. Cui, A. M. Asiri, G. Cui, B. Tang and X. Sun, *Nat. Commun.*, 2018, **9**, 3485.

33 Y. Zhang, W. Qiu, Y. Ma, Y. Luo, Z. Tian, G. Cui, F. Xie, L. Chen, T. Li and X. Sun, *ACS Catal.*, 2018, **8**, 8540–8544.

34 H. Huang, L. Xia, X. Shi, A. M. Asiri and X. Sun, *Chem. Commun.*, 2018, **54**, 11427–11430.

35 X. Zhu, Z. Liu, Q. Liu, Y. Luo, X. Shi, A. M. Asiri, Y. Wu and X. Sun, *Chem. Commun.*, 2018, **54**, 11332–11335.

36 L. Zhang, X. Ren, Y. Luo, X. Shi, A. M. Asiri, T. Li and X. Sun, *Chem. Commun.*, 2018, **54**, 12966–12969.

37 L. Ji, X. Shi, A. M. Asiri, B. Zheng and X. Sun, *Inorg. Chem.*, 2018, **57**, 14692–14697.

38 L. Xia, X. Wu, Y. Wang, Z. Niu, Q. Liu, T. Li, X. Shi, A. M. Asiri and X. Sun, *Small Methods*, 2018, **14**, 1800251.

39 H. Huang, L. Xia, R. Cao, Z. Niu, H. Chen, Q. Liu, T. Li, X. Shi, A. M. Asiri and X. Sun, *Chem. Eur. J.*, 2019, **25**, 1–5.

40 W. Kong, Z. Liu, J. Han, L. Xia, Y. Wang, Q. Liu, X. Shi, Y. Wu, Y. Xu and X. Sun, *Inorg. Chem. Front.*, 2019, **6**, 423–427.

41 R. Zhang, H. Guo, L. Yang, Y. Wang, Z. Niu, H. Huang, H. Chen, L. Xia, T.Li, X. Shi, X. Sun, B. Li and Q. Liu, *ChemElectroChem*, 2019, **6**, 1–6.

42 Z. Geng, Y. Liu, X. Kong, P. Li, K. Li, Z. Liu, J. Du, M. Shu, R. Si and J. Zeng, *Adv. Mater.*, 2018, **30**, 1803498.

43 Z. Wang, Y. Li, H. Yu, Y. Xu, H. Xue, X. Li, H. Wang and L. Wang, *ChemSusChem*, 2018, **11**, 3480–3485.

44 L. Huang, J. Wu, P. Han, A. M. AI-Enizi, T. M. Almutairi, L. Zhang and G.

Zheng, *Small Methods*, 2018, DOI: 10.1002/smtd.201800386.

45 X. Zhao, X. Lan, D. Yu, H. Fu, Z. Liu and T. Mu, *Chem. Commun.*, 2018, **54**, 13010–13013.

46 B. Xu, Z. Liu, W. Qiu, Q. Liu, X. Sun, G. Cui, Y. Wu and X. Xiong, *Electrochim. Acta*, 2018, **298**, 106–111.

47 K. Chu, Y. Liu, Y. Li, H. Zhang and Y. Tian, *J. Mater. Chem. A*, 2019, **7**, 4389–4394.

48 R. Zhang, L. Ji, W. Kong, H. Wang, R. Zhao, H. Chen, T. Li, B. Li, Y. Luo and X. Sun, *Chem. Commun.*, 2019, **55**, 5263–5266.